High Frequency Power Metamorphic HEMT

C. S. Whelan, K. Herrick, J. Laroche, K. W. Brown, F. Rose, Y. Zhang, P. Balas, R. E. Leoni III, W. E. Hoke, S. Lichwala, J. Kotce, T. E. Kazior

Raytheon RF Components
362 Lowell St. Andover, MA 01810, cwhelan@raytheon.com

***Abstract* - By tailoring the device's material, geometry and processing, our device designers have fabricated a state-of-the-art high frequency Metamorphic HEMT device with a G_{max} of 12 dB, a power density of 360 mW/mm, and PAEs exceeding 30% at 95 GHz. This device had been utilized to create a range of W-band amplifiers with excellent performance, including a 266 mW PA operating at 90 GHz.**

I. INTRODUCTION

GaAs based metamorphic HEMT (MHEMT) technology has emerged as an attractive, low cost alternative to InP HEMTs. The strain-induced imperfections caused by high indium content layers on GaAs are eliminated in metamorphic devices by providing a properly grown lattice-grading buffer between the substrate and active device layers. With this limitation overcome, it is now possible to provide the superior performance of InP-based devices with the cost advantages of highly manufacturable 4-inch GaAs wafers that can easily be integrated on existing GaAs fabrication lines [1]-[20].

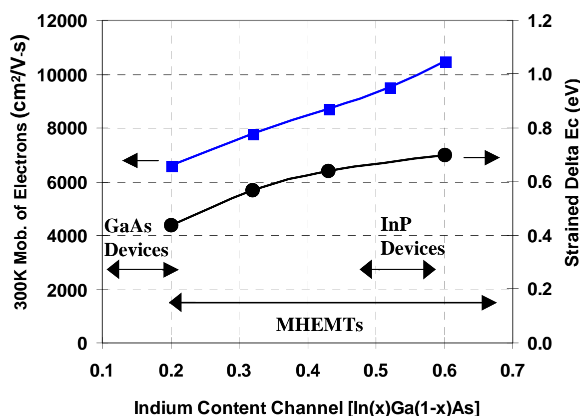

Figure 1. As indium is added to the channel, both the mobility and well depth increase (when a strained InAlAs layer is used).

We have fabricated metamorphic HEMT devices with channel indium contents ($In_xGa_{1-x}As$) ranging from 20% to 85% and measured such properties as band gap, mobilities, F_t, NF, gain, PAE, power densities and on- and off-state breakdown voltages. Figure 1 shows that the measured mobility of channel electrons increases with increasing channel In content, due mainly to the reduction in electron effective mass and reduced intervalley scattering (increasing E_L-E_{Gamma}). These improvements give rise to higher channel velocities, improving F_t. By straining the Schottky layer (with higher Al contents than lattice matched to $In_xGa_{1-x}As$), one can achieve improve confinement further, reducing NF and improving maximum current density (Figure 1). This collection of data has formed the basis to optimize a metamorphic GaAs HEMT for nearly any frequency and application.

We have successfully exploited the freedom of metamorphic device tailoring with our 4", 60% indium, low noise device technology that is currently in production. This paper describes a new pursuit and the results obtained by optimizing the material and processing to address the need for low cost, high gain, power amplifiers at W-band.

II. DEVICE AND PROCESSING

The MHEMT devices are mesa etched for isolation using a sulfuric based etchant. A series of metals containing Au/Ge are evaporated and annealed to form an ohmic contact, with contact resistance of approximately 0.17 Ohm-mm. Following ohmic formation, first recess and gate etching are performed selectively using a self-aligned gate method. 0.15 micron Ti/Pt/Au gates with wide T-tops (to reduce gate resistance) are then evaporated. Finally, silicon nitride is used to passivate the devices. The devices are thinned to 50 microns before being plated with gold. The devices employ individual source vias to reduce source inductance and improve thermal dissipation from the channel of the device.

The DC performance data for our new power MHEMT

device shows a G_m of 850 mS/mm, an I_{max} of 700 mA/mm, a V_{po} of –0.8V and a $V_{dg\ BRK}$ = 8V. The excellent uniformity of approximately 50 mV standard deviation in pinch off voltage across nearly (30) 4” wafers is due to both the high selectivity of the gate etch and the precision of the MBE growth process (Figure 2).

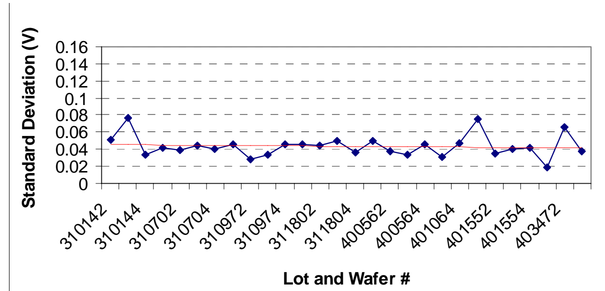

Figure 2. An average standard deviation of 50 mV is achieved across nearly (30) 4” wafers.

The materials layers of the Schottky and channel are carefully selected, with strain considerations, to optimized the high frequency performance of the devices, while maximizing on-state breakdown voltage. By exploiting metamorphic growth, the lattice constant of the device needs not be that of InP, thus giving the device designer a large degree of freedom in optimizing each material layer individually.

Pulsed IV data is overlaid upon static IV curves in Figure 3, and shows no current collapse, a necessity for achieving good power and efficiency. The device also demonstrates an I_{max} of 700 mA/mm and pulsed operation of up to 6V at 200 mA/mm. The high on-state breakdown (for a high indium content device) is achieved through channel recess optimization and material management to reduce impact ionization.

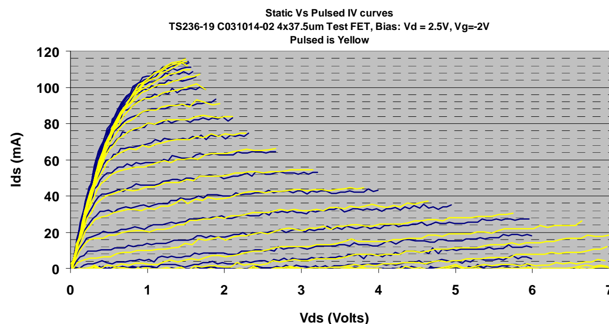

Figure 3. Pulsed IV overlaid upon static IV curves.

Figure 4 shows a G_{max} at 94 GHz of various geometry power MHEMT devices operating at 2V and approximately 300 mA/mm. As the devices scale to bigger peripheries with increasing gate fingers, the devices’ G_{max} only degrades by 1.5 dB. Due to optimized channel geometries, the devices lose virtually no gain as the unit gate width is increased from 37.5 microns to 60 microns. Even very large 8 finger x 60 micron unit gate width devices (480 micron total periphery) show 11 dB of maximum available gain at 94 GHz. This ability to scale is very promising for building large W-band power amplifiers with high gain per stage and efficiencies.

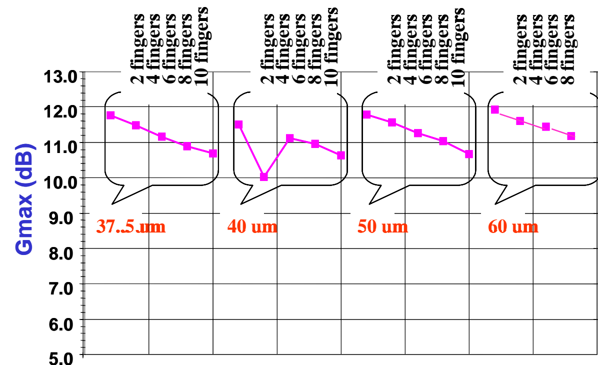

Figure 4. Gmax of power MHEMT devices biased at 2.0V at 94 GHz.

III. W-BAND AMPLIFIERS

Using our new power MHEMT material and device processing, we achieved state-of-the-art W-band power results. Single stage W-band pre-matched FETs with 150 microns of periphery were used to characterize the process and as building blocks for amplifier design.

S-parameters of these single stage pre-matched devices were taken on our 110 GHz ANA at 2.5V and 200 mA/mm and are shown in Figure 5. This 0.15 micron gate length power device shows 12 dB of measured gain at 104 GHz from a single stage.

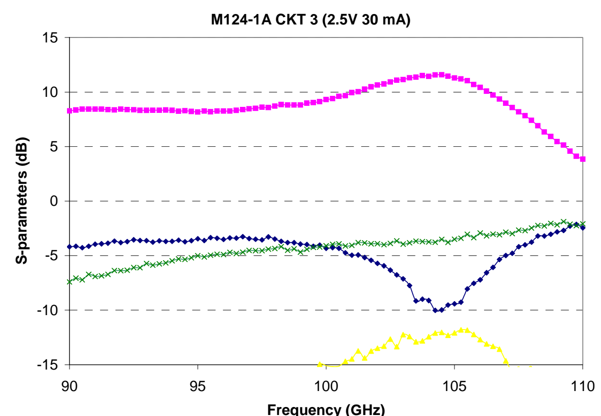

Figure 5. S-parameters of a single stage pre-matched device.

These same power matched devices were then measured for power at 95 GHz, as shown in Figure 6a. The 150 micron device shows a P_{sat} of 17.5 dBm with 27% power added efficiency and 5 dB of compressed gain (2.5 dB of compression). This equates to 360 mW/mm. This same circuit was biased for maximum PAE and produced 16 dBm of power and 32% PAE (Figure 6b). Load pull results of the same 150 micron device itself have yielded in excess of 35% PAE.

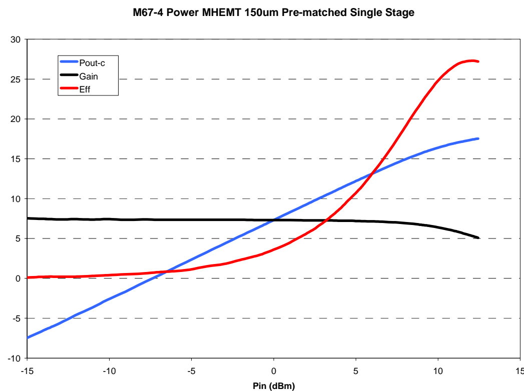

6a.

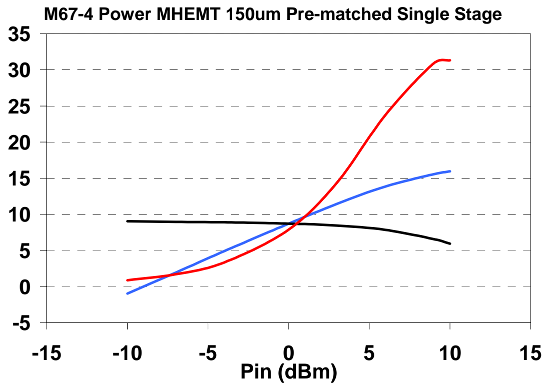

6b.

Figure 6a & b. Power, gain and efficiency of a 150 micron device measured at 95 GHz tuned for maximum power (a) and maximum PAE (b).

These single stage building blocks were used to create a large, single stage W-band power amplifier. Operating at a V_{ds} of 3.3V, the single stage PA demonstrated 6.5 dB of small signal gain, 17% PAE and 266 mW at 1 dB compression, all at 90 GHz (Figure 7).

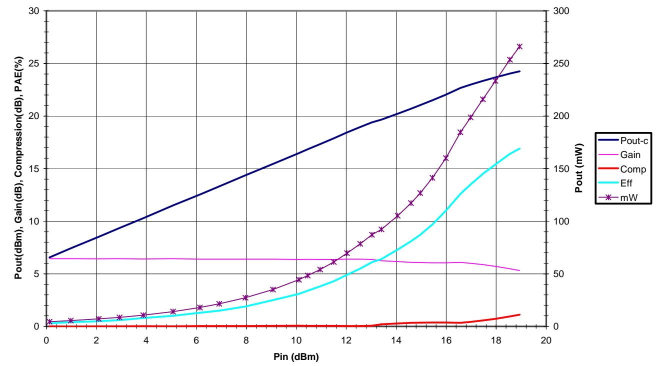

Figure 7. Power, gain and efficiency of a single stage, 90 GHz power amplifier.

V. CONCLUSION

A new power MHEMT process developed specifically for high frequency performance shows more than 12 dB of gain per stage at 100 GHz, 360 mW/mm power density and 30% power added efficiency at 95 GHz.

VI. REFERENCES

[1] "Raytheon, OMMIC launch new MHEMT processes," *Compound Semiconductor*, page 11, Oct. 2001.
[2] W.E. Hoke, et al., *JVST B* 17, p. 1131 (1999).
[3] D. Lubyshev, et al., *JVST B* 19, p. 1510, 2001.
[4] M. Chertouk et al, *IEEE EDL*, vol. 17, no. 6, p. 273-275, 1996.
[5] M. Kawano et al, *IEEE Microwave and Guided Wave Letters*, Vol. 7, No. 1, pp. 6-8, 1997.
[6] S. Halder, et al., *Proc. of 2001 Intern. Micro. Symp.*, p. 1885.
[7] W. K. Liu, *2001 InP and Related Materials Conf. Proc.*, p. 284.
[8] W.E. Hoke, et al., *JVST B* 19, p. 1505, 2001.
[9] P.M. Smith, et al., *Proc. of 2001 GaAs IC Symp.*, p. 7.
[10] A. Cappy, et al., *InP and Related Materials Conf. Proc.*, p. 192.
[11] P.F. Marsh et al., *Proc. of 2001 GaAs REL Workshop*, p. 119.
[12] M. Chertouk, et al., *2000 GaAs MANTECH Conf. Proc.*, p. 233.
[13] C.S. Whelan, et al, *2000 InP and Related Materials Conf. Proc.*
[14] C.S. Whelan, et al., *2001 CS-MAX Conf. Proc.*
[15] P. Balas, et al, *2002 CS-MAX Conf. Proc.*
[16] R. Leoni, et al, *2002 GaAs MANTECH Proc.*
[17] C. S. Whelan, et al, *2002 LEOS Conf. Proc.*
[18] P. Marsh, et al, *2003 TWHM Conf. Proc.*
[19] R. E. Leoni III, et al, *2003 GOMAC Conf. Proc.*
[20] K. Herrick, et al, *2003 MTT Conf Proc.*